Canadian Snow and Sea Ice: Trends (1981-2015) and Projections (2020-2050)

Lawrence Mudryk[1], Chris Derksen[1], Stephen Howell[1], Fred Laliberté[1], Chad Thackeray[2], Reinel Sospedra-Alfonso[3], Vincent Vionnet[4], Paul Kushner[5], and Ross Brown[6]

[1]Climate Research Division, Environment and Climate Change Canada, Toronto, Canada
[2]Department of Geography and Environmental Management, University of Waterloo, Canada
[3]Climate Research Division, Environment and Climate Change Canada, Victoria, Canada
[4]Centre National de Recherches Météorologiques, Centre d'Etudes de la Neige, Grenoble, France
[5]Department of Physics, University of Toronto, Toronto, Canada
[6]Climate Research Division, Environment and Climate Change Canada, Montreal, Canada

Correspondence to: Lawrence Mudryk (lawrence.mudryk@canada.ca)

Abstract. The Canadian Sea Ice and Snow Evolution Network (CanSISE) is a climate research network focused on developing and applying state of the art observational data to advance dynamical prediction, projections, and understanding of seasonal snow cover and sea ice in Canada and the circumpolar Arctic. Here, we present an assessment from the CanSISE network on trends in the historical record of snow cover (fraction, water equivalent) and sea ice (area, concentration, type, and thickness) across Canada. We also assess projected changes in snow cover and sea ice likely to occur by mid-century, as simulated by the Coupled Model Intercomparison Project Phase 5 (CMIP5) suite of earth system models. The historical datasets show that the fraction of Canadian land and marine areas covered by snow and ice is decreasing over time, with seasonal and regional variability in the trends consistent with regional differences in surface temperature trends. In particular, summer sea ice cover has decreased significantly across nearly all Canadian marine regions, and the rate of multi-year ice loss in the Beaufort Sea and Canadian Arctic Archipelago has nearly doubled over the last eight years. The multi-model consensus over the 2020-2050 period shows reductions in fall and spring snow cover fraction and sea ice concentration of 5-10% per decade (or 15-30% in total), with similar reductions in winter sea ice concentration in both Hudson Bay and eastern Canadian waters. Peak pre-melt terrestrial snow water equivalent reductions of up to 10% per decade (30% in total) are projected across southern Canada.

1 Introduction

Seasonal terrestrial snow and sea ice influence short term weather and longer term climate by altering the surface energy budget, modifying both the surface reflectivity and thermal conductivity (Serreze et al., 2007; Flanner et al., 2011; Gouttevin et al., 2012). Snow also influences freshwater storage through soil moisture recharge and surface runoff (Barnett et al., 2005). Understanding historical and projected future changes to snow and ice is essential both to assess the importance of physical changes to the climate system, and to thus assess their consequent impacts and risks. A previous assessment of the

Canadian cryosphere (snow, sea ice, freshwater ice, land ice, frozen ground) was compiled as part of the International Polar Year (IPY) in 2007-2008, and is described in Derksen et al. (2012). The current study updates the IPY analysis pertaining to terrestrial snow and sea ice by adding nearly a decade of data and including climate model projections of changes over the

35   next 30 to 40 years. This work is a core contribution of the Canadian Sea Ice and Snow Evolution Network (CanSISE), a climate research network focused on developing and applying state of the art observational data to advance dynamical prediction, projections, and understanding of seasonal snow cover and sea ice. Recognizing the critical importance of the snow/sea ice component of the cryosphere to Canada's natural environment, ecosystems, and economy, this CanSISE study focused on Canadian territory, which is nearly completely covered by snow and ice for parts of each year and which features

40   near-continuous coverage over high latitude and high elevation regions. While acknowledging the Canadian focus, much of the applied approach will be extended to other regions of interest through upcoming Coupled Model Intercomparison Project Phase 6 (CMIP6) experiments (i.e. van den Hurk et al., 2016).

Previous studies have shown that warming temperatures, which are amplified at higher latitudes as a natural response to

45   increasing greenhouse gases (Serreze et al., 2009; Pithan and Mauritsen, 2014), reduce the spatial extent and mass of snow and ice (for example, see Derksen et al., 2012). In reality, the linkage between warming temperatures and snow/sea ice reduction is more nuanced due to:

- *regional and seasonal climate variability*: for example, surface temperature warming across Canadian land and ocean areas is not uniform in space and time, but contains regional and seasonal variability driven by natural

50   climatic processes such as the El Niño Southern Oscillation (ENSO) and other oceanic teleconnections, and inter-seasonal and inter-annual changes in the preferred modes of atmospheric circulation (Vincent et al., 2015). The impact of warm temperature departures on the cryosphere vary with season: during spring they are directly linked to the timing and magnitude of melt onset; during fall warm temperatures can be associated with delayed snow cover onset and ice formation, the impacts of which may not become apparent for many months.

55   - *the selection of cryospheric variables*: the onset, accumulation/growth and melt of snow and sea ice are influenced by many factors and different metrics derived from these quantities that are relevant for different impacts on the environment and ecosystems do not always vary coherently with each other (Bokhorst et al., 2016). Changes in snow can be reflected in the timing of snow onset in the fall and melt in the spring, the peak seasonal accumulation of snow mass before melt, or the extent of snow covered area. For sea ice, not only are changes in the fractional ice

60   cover important but also the type of sea ice present, specifically whether it is thin first-year ice or thicker multi-year ice (Maslanik et al., 2011).

- *other process drivers*: while surface temperature plays a major role in influencing snow and ice, there are other important drivers of change. For instance, increased precipitation in sufficiently cold regions may offset shorter snow seasons (Brown and Mote, 2009). Sea ice dynamics (driven by wind and ocean currents) can play a major role

65   in regional sea ice conditions independent of surface temperature (Howell et al., 2013a).

- *snow/ice forcing of climate anomalies*: variations in snow and ice cover may also generate feedbacks to the atmosphere/ocean circulation that influence climate on seasonal to decadal scales (Cohen et al. 2007, Smith et al. 2010, Scaife et al. 2014), although there is no clear consensus on how changes in Arctic sea ice and snow cover influence midlatitude climate (Francis and Vavrus, 2012; 2015; Francis et al., 2017; Barnes, 2013; Screen et al., 2015).

The first objective of this paper is to provide an overview of observed changes to seasonal terrestrial snow and sea ice across Canadian territory using the longest available time series of validated gridded datasets. We use a multi-data set approach, averaging multiple estimates of terrestrial snow together for a more robust trend and using an integrated, multi-source dataset for analysis of sea ice change. The second objective is to compare these recent historical changes to projected changes of snow and sea ice over a similar length of time from the near future out to the middle of the 21st century (2020-2050). We use simulations from state of the art climate models with confidence levels that account for uncertainty in the regional temperature response (note that the focus of this study is not model evaluation – that analysis is described in Kushner et al., 2017). Results are presented in two sub-sections, separated by the observational analysis period (Section 3.1) and the future projections (Section 3.2). Details on the datasets and methodology are provided in Section 2. We summarize our key findings in Section 4 and present remaining points of discussion in Section 5.

2 Data

2.1 Historical Datasets

2.1.1 Terrestrial Snow Data

Following Mudryk et al. (2015), we took a multi-dataset approach to analyze observed snow cover change in order to account for observational uncertainty. We calculated monthly snow cover fraction (SCF) and seasonal maximum snow water equivalent (SWE) using daily SWE data taken from the following four sources over the 35 year period from 1981-2015. 1) The Modern-Era Retrospective Analysis for Research and Applications version 2 (MERRA-2), (Reichle et al., 2017, updated from Rienecker et al. 2011), is a National Aeronautics and Space Administration (NASA) atmospheric reanalysis product generated with the Goddard Earth Observing System Model, version 5.2.0 (GEOS-5) atmospheric general circulation model and atmospheric data assimilation system (ADAS). 2) The temperature index model described by Brown et al. (2003) reconstructs daily SWE using 6-hourly temperature field and 12-hourly precipitation field inputs from ERA-interim reanalysis. This simplified index model includes most of the temperature dependent processes included in the snow component of numerical land surface schemes (e.g., partitioning of precipitation into solid and liquid fractions, melt from rain-on-snow events, specification of new snowfall density, snow aging, and snowmelt). 3) The physical snowpack model Crocus simulates daily SWE using meteorology from ERA-Interim (Brun et al. 2013). 4) The European Space Agency

GlobSnow product (version 2; www.globsnow.info) is a gridded product derived through a combination of satellite passive microwave data, forward snow emission model simulations, and climate station observations for non-alpine regions of the northern hemisphere (Takala et al. 2011). Because the GlobSnow product is masked over complex topography, we replaced

100   such cells with a blend of the GlobSnow data and the mean value from the other three data sources. The weighting for the blend was determined by the fraction of the grid cell area containing complex topography. For grid cells with no complex topography, unaltered GlobSnow data are used. As the fraction of complex topography increases, the weight applied to the GlobSnow data is linearly reduced, reaching zero for grid cells only containing complex topography.

105   For a given dataset of daily SWE, we interpolated the data to a regular 0.25 degree grid over Canada and applied a 4 mm threshold to produce a daily binary snow cover extent. We averaged this daily field over each month to produce a monthly snow cover fraction. Seasonal maximum SWE fields were calculated as the maximum value of daily SWE attained at each grid location over a given snow season. For both SCF and maximum SWE, we computed trends separately for each of the four datasets and then averaged these together into a final trend representing the mean across the observational ensemble.

110   **2.1.2 Sea Ice Data**

We extracted total and multi-year ice (MYI) area within Canadian Arctic waters from the Canadian Ice Service Digital Archive (CISDA), which is an integration of a variety of data sets including: satellite observations, surface observations, airborne and ship reports, operational model results and the expertise of ice analysts (see Canadian Ice Service, 2007 and Tivy et al., 2011a for complete details). We selected the CISDA record instead of satellite passive microwave data because i)

115   the CISDA was found to be more accurate in the shoulder seasons during which passive microwave retrievals can underestimate sea ice concentration by as much as 44% (Agnew and Howell, 2003) and ii) the CISDA sea ice record provides homogeneous data back to 1968 for regions of the Canadian Arctic (Tivy et al., 2011a), almost 10 years earlier than coverage by satellite passive microwave observations. The CISDA data was analyzed over two historical periods, the 1981-2015 period consistent with available snow data and a longer 1968-2016 period.

120

We also used the Canadian Ice Service record of in situ landfast ice thickness measurements, made regularly at coastal Arctic stations since the early1950's (Howell et al. 2016b). In general, thickness measurements are available at weekly frequency, starting after freeze-up when the ice is safe to walk on and continuing until breakup or when the ice becomes unsafe. Details of this dataset are provided by Brown and Cote (1992) and are available on the Canadian Ice Service Web

125   site at http://iceglaces.ec.gc.ca.

2.1.3 Surface Temperature

In light of documented differences in gridded temperature datasets over Canada (Rapaic et al., 2015), surface temperature trends were derived from a blend of six reanalysis products: the European Centre for Mid-Range Weather Forecasting

(ECMWF) Reanalysis (ERA-Interim, Dee et al., 2011), the Japanese 55-year and 25-year Reanalyses (JRA-55, Kobayashi et
130   al., 2015; JRA-25, Onogi et al, 2007), the Modern-Era Retrospective analysis for Research and Applications version 1 and 2
(MERRA-1, Reinecker et al., 2011; MERRA-2, Reinecker et al., 2017), and the Climate Forecast System Reanalysis (CFSR,
Saha et al., 2010). The average trend was determined by first computing the average of JRA-55 and JRA-25 (resulting in a
single JRA trend), and the average of MERRA-1 and MERRA-2 (resulting in a single MERRA trend). The multi-reanalysis
mean trend was computed by averaging (ERA-Interim, CFSR, JRA, and MERRA). Reanalysis was used instead of point
135   station data in order to produce spatially continuous trends over both terrestrial and marine areas.

2.2 Model Simulations

2.2.1 Terrestrial Snow

We used monthly mean output from the suite of historical and future simulations from the CMIP5 archive (Taylor et al.
2012; http://cmip-pcmdi.llnl.gov/cmip5/) to evaluate snow cover fraction (variable 'SNC') and snow water equivalent
140   (variable 'SNW'). The models utilized for snow analysis are listed in **Table 1;** note that no model selection was performed –
all models with archived snow data were utilized. Future snow projections were selected from the Representative
Concentration Pathway (RCP) 8.5 projected forcing scenario because it most closely resembles the observed emissions
pathway over the past decade (Peters et al. 2013). We then computed individual trends for each realization and then took the
inter-realization average across each model to calculate individual model ensemble means. These values were averaged to
145   determine the CMIP5 multi-model mean values. If only a single realization was available, that was used directly as input to
the multi-model mean calculation. SWE and SCF output were also taken from a large initial condition ensemble (50
realizations) of the Second Generation Canadian Earth System Model (CanESM2; Arora et al., 2011), a global earth system
model from the Canadian Centre for Climate Modelling and Analysis. The realizations of this ensemble branch off from five
different historical simulations of CanESM2 in 1950, evolving under combined historical and RCP8.5 forcing scenarios in
150   accordance with CMIP5 (see Thackeray et al., 2016 for more details). This ensemble was used to characterize the role of
internal climate variability on projected snow cover changes over Canada.

2.2.2 Sea Ice

Monthly mean sea ice concentration (variable 'SIC') and the land-sea mask (variable 'SFTLOF') were also retrieved as
available from CMIP5 output resulting in a sea ice ensemble that comprises 42 models and a combined total of 91
155   simulations (Table 2). The sea ice concentration was projected to an EASE grid using the exact same procedure as in
Laliberte et al. (2016). For projections of sea ice-free conditions over the four Canadian marine subregions (Baffin Bay,
Beaufort Sea, Canadian Arctic Archipelago, and Hudson Bay), we excluded models that do not capture at least 75% of the
region's observed ocean area (resulting in about half of the models rejected in the Canadian Arctic Archipelago) and
compute sea ice extent (SIE), as in Laliberte et al. (2016).

2.3 Evaluation of Trend Significance

In order to make comparable significance calculations for the observed and projected trends, we use a Monte Carlo method following Swart et al. (2015) and applied in Howell et al. (2016). The method ensures that spread due to internal variability is comparable for all CMIP5 models, even those that only include a single realization in their archived output. This is achieved by adding simulated noise representing internal variability to those models with only a single realization. The added noise is calculated from the collection of models with multiple realizations under the assumption that the spread due to internal variability is the same across all models. A trend is significantly different from zero if it is distinguishable from the combined spread due to interannual variability (using a t-distribution for each simulation), internal variability (with noise added as described), and model spread.

We use an analogous approach to compute significance for the various observation-based dataset trends. We assume that differences in the trends arise from differences in retrieval performance and reanalysis methodologies but not from sampling of internal variability. Thus, a trend is significantly different from zero if it is distinguishable from the combined spread due to interannual variability (using a t-distribution for the dataset mean) and the added spread due to differences in the trends among the different data sets.

3 Results

3.1 Observed Trends in Terrestrial Snow and Sea Ice

Seasonally averaged trends in terrestrial snow cover fraction (SCF) and sea ice concentration (SIC) over the 1981-2015 time period are shown in **Figure 1** (the dashed line denotes limit of Canadian marine territory). Positive trends in SCF (more snow cover) are evident over a small region of the southern prairies in winter (January/February/March, JFM) and more extensively over western Canada in spring (April/May/June, AMJ). Trends in all remaining regions and seasons are negative, notably over eastern Canada in spring and most of the Canadian land area in the fall (October/November/December, OND). The predominantly negative trends in snow cover are consistent with previous studies (Brown and Braaten, 1998; Vincent et al. 2015) but with evidence of a shift to stronger snow cover reductions in the snow onset period over eastern Canada in response to enhanced OND warming shown in **Figure 2 (discussed below)**. The observed rates of snow cover change are also consistent with the recent Snow, Water, Ice, Permafrost in the Arctic (SWIPA) assessment (Brown et al. 2017) that documented annual SCD changes over Arctic land areas of -2 to 4 days/decade (~ -1 to -2% per decade assuming 250 days mean snow cover). Other studies focused on Arctic snow cover (i.e. Derksen and Brown, 2012; Derksen et al., 2016) have identified spring snow cover losses that are stronger than those in **Figure 1.** This difference may stem from stronger spring trends in the NOAA snow chart data record (the NOAA dataset was not used in this study due to known deficiencies in the

fall period; Brown and Derksen, 2013) compared to other snow products (Mudryk et al., 2017), and stronger trends across the Eurasian Arctic compared to North America (Derksen et al., 2016).

SIC trends over Canadian waters for this period are almost exclusively negative in all seasons. Regions with the strongest SIC declines are eastern Canadian waters in winter and spring, and the Canadian Arctic Archipelago and Hudson Bay in summer and fall consistent with the warming patterns shown in Figure 2. The SCF and SIC trends can be viewed collectively as changes in the timing and extent to which highly reflective snow and ice cover the Earth's surface, with important implications for the surface energy budget. There are no sharp boundaries in trends across adjacent land and ocean regions. This provides confidence in the consistency of the snow and ice datasets, as well as evidence of a coherent response of snow and ice to temperature forcing across terrestrial and marine regions.

Figure 2 shows seasonal surface air temperature (TAS) trends over the 1981-2015 period computed from a blend of six atmospheric reanalysis datasets (see Section 2.1.3). TAS trends are generally positive, although no trends are seen throughout the northwestern portion of the country during winter and spring, and there is significant cooling over the Canadian prairies in spring. Land areas with cooling trends are co-located with positive SCF trends in **Figure 1**, although the region with positive SCF trends is slightly more extensive. The reduced warming and cooling over northwestern Canada is consistent with the influence of North Pacific oceanic variability over the last 35 years as analyzed in Mudryk et al., 2014. The reanalysis TAS trends are also seasonally and spatially consistent with the analysis of Rapaic et al. (2015, Fig. 13) based on blended data from both homogenized station observations and multiple reanalyses. In both reanalysis and in situ data, Arctic trends are strongest in the fall and winter, with an increase in the magnitude of warming from the southwest to northeast regions of the country apparent in all seasons.

To examine the role of air temperature trends in driving the observed snow and ice cover trends, spatial correlations (centered and uncentered) were calculated to quantify the pattern relationship between SCF, SIC, and TAS trends (**Figure 3**). The centered (uncentered) statistic measures the similarity of the two patterns after (without) removal of the domain mean. A large negative uncentered correlation indicates that the correlation between the two fields is negative on average, but does not require that the field patterns are congruent. A large negative centered correlation does require spatial similarity in the field patterns. Both SCF and SIC trend show large uncentered correlations for all seasons indicative of the general relationship between increasing temperatures and decreasing SCF and SIC. During JFM and AMJ, the large centered correlations between SCF and TAS indicate that the spatial patterns are also similar, and hence there is a strong association between SCF and TAS trends at the local scale during these seasons, with reduced connections during JAS and OND (consistent with Mudryk et al, 2017). SIC trend patterns are more closely associated with warming patterns during ice onset/growth (OND and JFM), however overall there is less co-variability of SIC trends with TAS trends than for SCF trends. This difference may stem from the fact that ice (especially MYI) is more difficult to melt than snow, and the

additional influence of dynamical effects (such as wind-driven redistribution of sea ice) weakens the thermodynamically
225 driven spatial association between SIC and TAS trends.

Trends in pre-melt seasonal maximum snow water equivalent (SWEmax), which indicates water resource and streamflow
potential just before spring melt, are shown in **Figure 4.** The figure represents averages from the same datasets used to
generate the SCF trends in **Figure 1**. Trends are negative over much of Canada, indicating a reduction over time in SWEmax
230 at the onset of the melt season each spring. This is consistent with observed in situ snow depth trends (Brown and Braaten
1998; Vincent at al., 2015) and other observational studies (for example Mudryk et al., 2015). There is evidence of SWEmax
increases in the western Canadian Arctic Archipelago (CAA) but these are modest in strength and regionally limited. As will
be discussed further in Section 4 in the context of future projections, the varying influence of temperature and precipitation
changes need to be disentangled in order to understand the driving mechanisms behind trends in SWEmax (Raisanen, 2008;
235 Brown and Mote, 2009).

The longer period of consistent summer sea ice information in Canadian waters from the CISDA allows consideration of
additional years not covered by the 1981-2015 trends in **Figure 1**. To be consistent with Tivy et al. (2011a) and Derksen et
al., (2012) the summer is ice season is defined as average sea ice area from June 25 to October 15 for the Beaufort Sea,
240 CAA, and Baffin Bay regions and from June 18 to November 19 for Hudson Bay, Hudson Strait, Davis Strait and Labrador
Sea. Between 1968 and 2016, sea ice area averaged over the summer period has experienced significant decreases in almost
every region of the Canadian Arctic, up to 20% per decade in some regions (e.g. the Hudson Strait and Labrador Sea; **Figure
5**). Compared to previous trends reported by Tivy et al. (2011a) over the period of 1968-2008 and Derksen et al., (2012) for
1968-2010, more regions are now experiencing significant decreases and the rate of decline is stronger in all regions except
245 Hudson Bay (**Figure 6e**). For MYI, there are more regions across the Canadian Arctic, particularly in the western CAA, that
are now experiencing significant declines compared to previous studies (e.g. Tivy et al., 2011a; Derksen et al., 2012; **Figure
5**). The largest declines in MYI occurred in the CAA and Beaufort Sea, both of which almost doubled their rate of decline
for 1968-2016 when compared to the trend for 1968-2008 (**Figure 6e**).

250 A stepwise reduction in Hudson Bay sea ice area occurred in the mid-1990s (**Figure 6d**; Tivy et al., 2011b; Hochheim and
Barber, 2014) and Baffin Bay has experienced consistently low sea ice area since 1999 (**Figure 6c**); whereas, considerably
more interannual variability is apparent in the Beaufort Sea and CAA (**Figures 6a and b**). Of note, the Beaufort Sea
experienced a record low sea ice area in 2012, becoming virtually ice-free near the end of the melt season (Babb et al.,
2016). This was nearly repeated in 2016. As previously reported, the CAA eclipsed the previous and long standing record
255 low ice year of 1998 in both 2011 and 2012 (Howell et al., 2013b). A contributing factor to the decline of sea ice across the
Canadian Arctic is increasing spring air temperature (see **Figure 2**) coupled with longer melt seasons resulting in the

absorption of more solar radiation and increased ice melt (Howell et al., 2009; Tivy et al., 2011a; Stroeve et al., 2014; Parkinson, 2014).

260   Arctic sea ice thickness has declined in recent years (e.g. Kwok and Rothrock, 2009; Haas et al., 2010; Laxon et al., 2013; Richter-Menge and Farrell, 2013; Kwok and Cunningham, 2015; Tilling et al., 2015). These studies indicate thickness declines are greater in the Beaufort Sea compared to the north facing coast of the CAA, which still contains some of the thickest sea ice in the world. Unfortunately, the spaceborne sensors used to obtain sea ice thickness information are not of sufficient spatial resolution to provide reasonable thickness estimates within the CAA. However, the Canadian Ice Service

265   record of in situ landfast ice thickness measurements represents one of the longest datasets in the Arctic, and spans over 5 decades (Howell et al., 2016b). However, the seasonal behaviour of landfast ice thickness can provide useful information for understanding the interannual variability because ice growth is almost entirely due to thermodynamic forcing. Significant declines in maximum ice thickness have occurred at 3 sites in the CAA (Cambridge Bay, Eureka, and Alert) with decreases ranging between -3.6 to -5.1 cm per decade over the period from the late 1950s to 2016 (**Figure 7**). No significant trend was

270   found at Resolute (**Figure 7b**) but an early study from Brown and Cote (1992) reported a significant increase in maximum ice thickness at Resolute over the period from 1950-1989.

Although systematic measurements at other regions within the CAA are unavailable or contain too much uncertainty, surveys in 2011 and 2014 of ice thickness from airborne electromagnetic induction (AEM) described by Haas and Howell

275   (2015) indicated the ice is still thick, with a modal thickness of 1.8-2.0 m (not shown). Ice between 3-4 m in mean thickness was found in the MYI regions throughout the CAA.

3.2 Projected Changes in Terrestrial Snow and Sea Ice

Projected trends in snow cover fraction (SCF) and sea ice concentration (SIC) for the 2020-2050 time period across Canadian territory are shown in **Figure 8**. These projections are the multi-model mean from the ensemble of CMIP-5 climate

280   models, using the RCP8.5 forcing scenario (which assumes 'business as usual' continued growth of greenhouse gas emissions through the 21st century). While other scenarios exist, projections to the mid-century are primarily dependent on natural variability and model dependent uncertainties rather than the choice of forcing scenario (Hodson et al., 2012). The multi-model projected mean changes in surface temperature are positive in all seasons, hence in the ensemble mean only reductions in SCF and SIC are evident in **Figure 8**. Seasonal differences and varying sensitivity of snow and ice to

285   temperature forcing drives the spatial variability in **Figure 8**. During winter, projected snow cover reductions are greatest along the southern margins of Canada, where temperature increases directly result in less snow. Temperatures remain sufficiently cold at higher latitudes (despite projected warming) so there is no projected response in this region in JFM SCF. During spring, the region of snow sensitivity to temperature forcing shifts north, across the boreal forest, subarctic, and Arctic tundra, which leads to the negative SCF trends projected across these regions during AMJ. Ensemble-mean reductions

projected for SIC are very strong and focused on the ice melt (summer) and ice formation (fall) seasons, with the exception of Hudson Bay and eastern Canadian waters which also have projected winter season loss of sea ice cover.

While natural decadal-scale climate variability resulted in cooling trends (and hence positive SCF and SWEmax trends) for some regions and seasons during the 1981-2015 period (see **Figures 1, 2 and 4**), over the longer 1948-2012 period observed surface temperature trends over Canada are almost exclusively positive (Vincent et al., 2015). Similarly, we expect there could be short term, localized fluctuations in trend direction and magnitude from the projections shown in **Figure 8**. These localized fluctuations exist in individual realizations of the model projections (not shown) and act to increase the spread in the TAS, SCF, and SIC responses. This spread reduces the significance of the ensemble-mean response for a given confidence level; for this reason only the coastal regions in British Columbia show significant SCF decreases at the 90% confidence level, whereas projections show widespread reductions in SIC at the 90% confidence level. The differences between SCF and SIC in the significance of their projected responses may result from varying sensitivity to temperature forcing if SCF depends more strongly on the local temperature response than SIC.

Figure 9 shows trends in SWEmax also derived from the CMIP-5 multi-model ensemble. The ensemble mean shows that peak SWEmax loss will be extensive (5-10% per decade through 2050, or a cumulative 15-30% reduction over the entire 2020-2050 period) over much of Alberta and British Columbia, and similarly in Southern Ontario and the Maritime provinces (note that the greatest near-future loss in the CMIP5 ensemble occurs just south of the Canadian border, not shown in **Figure 9**). While positive Arctic SWEmax trends start to emerge by mid-century in the Eurasian Arctic (not shown; see Brown et al., 2017) minimal change is projected across high latitude land areas of Canada because increasing temperature (which shortens the snow accumulation season) balances projected increases in snowfall.

Month by month projected changes in Canadian snow extent and snow mass for the CMIP5 multi-model ensemble, and the large initial condition ensemble from the second generation Canadian Earth System Model (CanESM2) are shown in **Figure 10**. The two ensembles agree that the greatest near-future snow loss (as a percentage of climatological snow) is projected to occur in the shoulder seasons (Oct-Nov, May-Jun). During mid-winter there is minimal percentage change in snow cover extent projections because winter temperatures over northern regions of Canada will remain cold enough to sustain snow cover and there is greater climatological snow extent in winter, which results in smaller percentage changes reflected in **Figure 10**. The projected trends from CMIP5 are similar in magnitude to the rate of change during the historical period considered in this study, while trends from CanESM2 are slightly stronger due to greater warming in CanESM2 compared to the CMIP5 multi-model mean (Thackeray et al., 2016). Because the CMIP5 ensemble includes many different models, there is a greater spread in most months than the CanESM2-LE, which represents multiple climate realizations generated from a single model. Nonetheless, it's striking that the interquartile range of the CanESM Large Ensemble is quite comparable to

that of the CMIP model ensemble. This likely indicates that a large portion of the inter-model spread is associated with internal variability.

325

Sospedra-Alfonso and Merryfield (2017) showed that the interannual variability in monthly SWE between January and April can be skillfully estimated with a multiple linear regression model based on precipitation and temperature predictors. This statistical model suggests coherent relationships that provide context to the character of the changes to terrestrial snow cover that are being considered here. **Figure 11** shows present-day (1981-2016) and projected (2015-2050) seasonal near-surface
330 air temperature (T_s) defined following Sospedra-Alfonso and Merryfield (2017) and given roughly by the average temperature over the consecutive months from snow onset up to March. Results are obtained from five ensemble members of historical (1951-2005) + RCP8.5 (2005-2100) simulation runs in CanESM2 downscaled with CanRCM4. The seasonal temperature threshold, T_{th}, divides March snow cover into two regions characterized by their sensitivity to precipitation and temperature variability; the region where $T_s < T_{th}$ has snowpack variability driven mainly by precipitation, whereas the region
335 where $T_s > T_{th}$ has temperature-driven snowpack variability. The temperature threshold is temporally varying but is generally found between T_{th}=-5±1°C for historical and projected simulations. This range is in agreement with Sospedra-Alfonso and Merryfield (2017) who showed that T_{th} in CanESM2 is largely independent of time and emission scenario.

In 1981-2016, regions with temperature-dominated March snowpack ($T_s \gtrsim$-5°C) include coastal British Columbia, southern
340 Alberta, southwest Saskatchewan, southern margins of the St. Lawrence River and the Great Lakes, the Maritime provinces and Newfoundland. Because of the projected warming, the seasonal isotherms shift northward and toward higher elevations extending the portion of the snow cover that is more sensitive to temperature variations. By 2015–2050, regions with temperature-driven snowpack also include most of southern Canada, the interior of British Columbia, and more extensive portions of the Prairies provinces, Ontario and Quebec. In these regions, March SWE is expected to decrease during
345 anomalously warm years. The portion of the snow cover with $T_s <$-20°C, which is largely unaffected by temperature variability (Sospedra-Alfonso and Merryfield, 2017) and encompasses areas of the Northwest Territories and most of Nunavut in present-day climate, is projected to recede to the Canadian Archipelago by mid-century.

Turning to projected changes in sea ice, **Figure 12** shows the observed record of sea ice extent (sea ice concentration >15%)
350 across Canadian marine regions, compared to the CMIP-5 multi-model ensemble. While the observed and simulated trends are similar, only those years with strong observed negative departures from the long term trend (e.g. 1998 and 2012) reach the mean simulated ice extent. During the historical record, the models have a large spread (gray histogram, right side of **Figure 12**), with most models within the range of observations. After 2050, the large spread persists, but most models are ~10% below the historical sea ice extent (yellow histogram, right side of **Figure 12**).

355

The probability of sea ice free conditions by 2050 for regions of the Canadian Arctic calculated from the CMIP-5 multi-model ensemble are shown in **Figure 13** (see Laliberté et al., 2016, for a full description of the sea ice free probability methodology). Use of two ice area thresholds, 5% and 30%, applied to each grid cell, indicates the sensitivity in timing to the definition of minimum ice area. Under a 5% ice area scenario, there is a greater than 50% probability that all Canadian
360 regions will be sea ice free in September. Ice free probabilities are similar for August, but lower for October and November. Hudson Bay, which is already largely ice free in August and September, has a high probability of being ice free for 4 consecutive months. With a more relaxed threshold of 30% ice area, probabilities are (by definition) greater for all regions and months. Baffin Bay is projected to be ice free for August through October, and 2 months of ice free conditions in the Beaufort Sea and the CAA are a possibility.

4 Key Findings

This assessment of observed historical changes in terrestrial snow cover and sea ice over Canada, together with projected changes to the middle of the 21st century, has produced the following key findings:

Historical datasets show the fraction of Canadian land and marine areas covered by snow and ice is decreasing.
370 Observations show decreased SIC in all seasons and decreased terrestrial SCF in fall (delayed snow cover onset) and spring (earlier snow melt). There is regional and seasonal variability in the direction and strength of the trends (for example, some increases in spring snow cover across boreal western Canada) due to seasonal and spatial variability in surface temperature trends resulting from natural climate variability. There is evidence of decreasing pre-melt SWE (reflective of shallower snow depth) consistent with the study of Mudryk et al. (2015) and trends of annual maximum snow depth reported in Vincent et al.
375 (2015). There is only regional evidence (western CAA) of increasing winter season snow accumulation and hence higher SWE across Arctic Canada. Summer season total ice cover is decreasing significantly across nearly all Canadian marine regions. MYI ice losses are greatest in the Beaufort Sea and the western CAA. In just 8 years, the rate of MYI loss nearly doubled over the 1968-2016 period, compared to a previous assessment over 1968-2008. 60 year long records of in situ landfast ice thickness show evidence of thinning ice in the CAA that was not evident in an earlier study by Brown and Cote
380 (1992), which covered the late 1950s to 1989.

Canadians should anticipate further reductions in snow and sea ice cover by the middle of the 21st century.
Averaging projections across many climate model simulations provides evidence that SCF, pre-melt peak SWE, and SIC will continue to decrease across Canadian land and marine areas through the middle of the 21st century. However, this decrease
385 need not be spatially uniform and regions of negligible decrease or even increase are possible in the near future due to climate variability competing with anthropogenic forcing at the decadal and multi-decadal time scale. For the highly populated regions of southern Canada, there is evidence of a shift in the primary control on inter-annual variability in snow

cover from precipitation availability to surface temperature. While the thickest sea ice in the world will continue to be present in the CAA and along its northern coast, climate models suggest that Canadian Arctic marine regions which are
390 currently ice covered could be sea ice-free in the summer by 2050.

5 Discussion

Snow cover is a defining characteristic of the Canadian landscape for a few months each winter along the southern margins of the country and up to 9 or 10 months each year in the high Arctic, evolving from nearly complete snow cover over the entire country in the winter to a near total loss of snow cover by the summer. Highly reflective snow cover acts to cool the
395 climate system, effectively insulates the underlying soil, and stores and redistributes water in solid form through the accumulation season before spring melt. Sea ice insulates the ocean from the atmosphere; provides an essential habitat for northern mammals, influences navigation and access to the north, and is of high importance to the traditional lifestyle of northern communities. This assessment of observed and projected changes in seasonal terrestrial snow and sea ice is focused on Canadian territory, but a number of cross-cutting issues with broader implications for understanding interactions between
400 the cryosphere and climate system were identified through this analysis:

1. The majority of previous assessments of snow cover trends (i.e. Derksen and Brown, 2012; Hernandez-Henriquez et al, 2015; Derksen et al., 2016; Kunkel et al., 2016) were based on the NOAA snow chart climate data record (NOAA-CDR; Estilow et al., 2015) selected on the basis of the longest available record. The reliance on individual datasets such as the
405 NOAA-CDR, however, makes trends prone to uncertainty due to the inherent uncertainties in an individual dataset (for instance, see Brown and Derksen, 2013 and Mudryk et al., 2017 for issues related to the NOAA-CDR). It is clear that consideration of multiple datasets either as a means of showing the range of trends from individual datasets (Mudryk et al., 2017), for calculating confidence intervals around an individual dataset (Brown and Robinson, 2011), or to benchmark other datasets (Brown et al., 2010; Hori et al., 2017) is a more robust approach. However, in this case, we acknowledge that the
410 availability and use of multiple datasets came at the sacrifice of time series length (the NOAA record extends back to 1967, whereas passive microwave satellite data and reanalyses such as ERA-interim only begin in 1979).

2. Alpine snow poses a unique challenge to trend analysis because the coarse spatial resolution of gridded products used for climate analysis cannot resolve the high degree of spatial variability (driven by land cover variability and steep topographic
415 gradients) in alpine regions. It is imperative that we address and improve our ability to characterize variability and change in alpine snow because it is these regions that are both extremely sensitive to climate induced changes in snow accumulation (i.e. elevation dependent changes in rainfall versus snowfall ratios) and impactful with respect to water resources (Fyfe et al., 2017; Berg and Hall, 2017; Sospedra-Alfonso et al., 2015; Scalzitti et al., 2016).

420   3. Changes in sea ice are driven by warming temperatures, but also by changes in atmospheric circulation. The Beaufort Sea was once a region where ice would thicken and age before being transported to the Chukchi Sea and re-circulated in the Arctic (Tucker et al., 2001; Rigor et al., 2002) but now the region has become a considerable contributor to the Arctic's MYI loss (Kwok and Cunningham, 2010; Maslanik et al., 2011; Krishfield et al., 2014; Galley et al., 2016). Ice is still being sequestered from the Canadian Basin and transported through the Beaufort Sea during the summer months but the ice is now

425   younger and thinner and unable survive the melt season en route to the Chukchi Sea (Howell et al., 2016a). The CAA was also a region with historically heavy MYI conditions present throughout the melt season but ice conditions have become lighter in recent years (see **Figure 6b**). The replenishment of CAA MYI via FYI aging and MYI inflow from the Arctic Ocean has decreased in recent years because of increased temperature and changes in atmospheric circulation (Howell et al., 2015).

430

4. There is a strong association between the magnitude of warming and snow and ice loss both in observational datasets and climate model simulations, with projected declines in snow and sea ice cover proportional to the amount of future warming (Thackeray et al., 2016; Mudryk et al., 2017; Notz and Stroeve, 2016). The multi-model mean projections indicate decreasing snow and ice cover because the multi-model mean projects a warmer climate by mid-century. Within this multi-

435   model mean, however, individual climate model realizations contain regions and seasons with cooling trends (see Mudryk et al., 2014). It is important to remember, therefore, that we live in a single climate realization, while models produce dozens of potential realizations of a future climate. The multi-model mean warming trend (with associated reductions in snow and ice cover) is indicative of a high likelihood of a warmer future, but there will be decadal-scale natural variability, particularly at regional scales, projected onto this overall trend.

440

The objective of this report was to provide a physical climate assessment of observed and projected changes in snow and ice across Canada. While not the focus of this study, these changes will have profound impacts on terrestrial and marine ecosystems, and many sectors of the Canadian economy. This includes risks related to freshwater supply from snow (Sturm et al, 2017) and other impacts of changing snow on the Canadian landscape and economy (Sturm et al., 2016). Resolving the

445   dates of summer sea ice-free conditions for Canadian regions (Laliberté et al. (2016) has important implication for climate studies, but also for determining impact and mitigation strategies. The decreases in MYI within the Beaufort Sea and the CAA illustrated in **Figure 5** were found to be statistically linked to an increase in shipping activity, pointing out the potential implications of continued sea ice declines in these regions (Pizzolato et al., 2016).

References

450   Agnew, T., and S. Howell: The use of operational ice charts for evaluating passive microwave ice concentration data, Atmos. Ocean, 41, 317–331, doi:10.3137/ao.410405, 2003.

Arora, V. K., Scinocca, J. F., Boer, G. J., Christian, J. R., Denman, K. L., Flato, G. M., Kharin, V. V., Lee, W. G., and Merryfield, W. J.: Carbon emission limits required to satisfy future representative concentration pathways of greenhouse gases, Geophys. Res. Lett., 38, 3–8, doi:10.1029/2010GL046270, 2011.

455 Babb, D. G., Galley, R. J., Barber, D. G., and Rysgaard, S.: Physical processes contributing to an ice free Beaufort Sea during September 2012, J. Geophys. Res. Oceans, 121, 267–283, doi:10.1002/2015JC010756, 2016.

Barnes, E.: Revisiting the evidence linking Arctic amplification to extreme weather in midlatitudes, Geophys. Res. Lett., 40, 4734–4739, doi:10.1002/grl.50880, 2013.

Barnett, T., Adam, J., and Lettenmaier, D.: Potential impacts of a warming climate on water availability in snow-dominated
460 regions. Nature. 438, 303-309, doi:10.1038/nature04141, 2005.

Berg, N., and Hall, A.: Anthropogenic warming impacts on California snowpack during drought, Geophys. Res. Lett., 44, 2511-2518, doi:10.1002/2016GL072104, 2017.

Bokhorst, S., et al.: Changing Arctic snow cover: A review of recent developments and assessment of future needs for observations, modelling, and impacts, Ambio, DOI 10.1007/s13280-016-0770-0, 2016.

465 Brown, R. D., and Braaten, R. O.: Spatial and temporal variability of Canadian monthly snow depths, 1946-1995. Atmosphere-Ocean, 36, 37-45, 1998.

Brown, R. and Cote, P.: Interannual variability of landfast ice thickness in the Canadian high arctic, 1950–89, Arctic, 45, 273–284, 1992.

Brown, R., Brasnett, B., and Robinson, D.: Gridded North American monthly snow depth and snow water equivalent for
470 GCM evaluation, Atmos.-Ocean. 41, 1-14, 2003.

Brown, R., and Mote, P.: The response of Northern Hemisphere snow cover to a changing climate, J. Clim., 22, 2124-2145, 2009.

Brown, R., Derksen, C., and Wang, L.: A multi-dataset analysis of variability and change in Arctic spring snow cover extent, 1967-2008. J. Geophys. Res., 115, D16111, doi:10.1029/2010JD013975, 2010.

475 Brown, R., and Robinson, D.: Northern Hemisphere spring snow cover variability and change over 1922–2010 including an assessment of uncertainty. Cryosphere, 5, 219–229, doi:10.5194/tc-5-219-2011, 2011.

Brown, R., and Derksen, C.: Is Eurasian October snow cover extent increasing? Env. Res. Lett., 8, 024006 doi:10.1088/1748-9326/8/2/024006, 2013.

Brown, R., Schuler, D., Bulygina, O., Derksen, C., Luojus, K., Mudryk, L., Wang, L., and Yang, D.: Arctic terrestrial snow.
480 In Snow, Water, Ice and Permafrost in the Arctic (SWIPA). Arctic Monitoring and Assessment Program, 2017.

Brun, E., Vionnet, V., Boone, A., Decharme, B., Peings, Y., Valette, R., Karbou, F., and Morin, S.: Simulation of Northern Eurasian local snow depth, mass, and density using a detailed snowpack model and meteorological reanalyses, J. Hydrometeor., 14, 203–219, doi:10.1175/JHM-D-12-012.1, 2013.

Canadian Ice Service: Regional charts: History, accuracy, and caveats, Arch. Doc. Ser. 1, Ottawa. [Available at http://ice.ec.gc.ca/IA_DOC/cisads_no_001_e.pdf.], 2007.

Cohen, J., M. Barlow, P.J. Kushner, and K. Saito: Stratosphere–Troposphere Coupling and Links with Eurasian Land Surface Variability. *J. Climate,* **20**, 5335–5343, doi:10.1175/2007JCLI1725.1, 2007.

Dee, D. P., Uppala, S. M., Simmons, A. J., Berrisford, P., Poli, P., Kobayashi, S., Andrae, U., Balmaseda, M. A., Balsamo, G., Bauer, P., Bechtold, P., Beljaars, A. C. M., van de Berg, L., Bidlot, J., Bormann, N., Delsol, C., Dragani, R., Fuentes, M., Geer, A. J., Haimberger, L., Healy, S. B., Hersbach, H., Hólm, E. V., Isaksen, L., Kållberg, P., Köhler, M., Matricardi, M., McNally, A. P., Monge-Sanz, B. M., Morcrette, J.-J., Park, B.-K., Peubey, C., de Rosnay, P., Tavolato, C., Thépaut, J.-N. and Vitart, F.: The ERA-Interim reanalysis: configuration and performance of the data assimilation system. Q.J.R. Meteorol. Soc., 137: 553–597. doi: 10.1002/qj.828, 2011.

Derksen, C., et al.: Variability and change in the Canadian Cryosphere, Clim. Change, 115(1), 59–88, 2012.

Derksen, C., Brown, R., Mudryk, L., and Luojus, K.: Terrestrial Snow (Arctic). In State of the Climate in 2015, Bull. Am. Met. Soc., 97, S145-S147, 2016.

Estilow, T. W., Young, A. H., and Robinson, D. A.: A long-term Northern Hemisphere snow cover extent data record for climate studies and monitoring, Earth Sys. Sci. Data, 7.1, 137-142, 2015.

Flanner, M., Shell, K., Barlage, M., Perovich, D., and Tschudi, M.: Radiative forcing and albedo feedback from the Northern Hemisphere cryosphere between 1979 and 2008. Nature Geosci., 4, 151–155, doi:10.1038/ngeo1062, 2011.

Francis, J., and Vavrus, S.: Evidence linking Arctic amplification to extreme weather in mid-latitudes. Geophys. Res. Lett., 39, L06801, doi:10.1029/2012GL051000, 2012.

Francis, J., and Vavrus, S.: Evidence for a wavier jet stream in response to rapid Arctic warming. Env. Res. Lett., 10, doi:10.1088/1748-9326/10/1/014005, 2015.

Francis, J., Vavrus, S., and Cohen J.: Amplified Arctic warming and mid-latitude weather: new perspectives on emerging connections. WIREs Clim. Change, e474, doi: 10.1002/wcc.474, 2017.

Fyfe, J., Derksen, C., Mudryk, L., Flato, G,. Santer, B., Swart, N., Molotch, N., Zhang, X., Wan, H. Arora, V., Scinocca, J., and Jiao, Y: Large near-term projected snowpack loss over the western United States, Nature Comms., 10.1038/NCOMMS14996, 2017.

510 Galley, R. J., Babb, D., Ogi, M., Else, B. G. T., Geilfus, N.-X., Crabeck, O., Barber, D. G. and Rysgaard, S.: Replacement of multiyear sea ice and changes in the open water season duration in the Beaufort Sea since 2004, J. Geophys. Res. Oceans, 121, 1806–1823, doi:10.1002/2015JC011583, 2016.

Gouttevin, I., Menegoz, M., Dominé, F., Krinner, G., Koven, C., Ciais, P., Tarnocai, C., and Boike, J.: How the insulating properties of snow affect soil carbon distribution in the continental pan-Arctic area, J. Geophys. Res., 117, G02020,
515 doi:10.1029/2011JG001916, 2012.

Haas, C., Hendricks, S., Eicken, H., and Herber, A.: Synoptic airborne thickness surveys reveal state of Arctic sea ice cover, Geophys. Res. Lett., 37, L09501, doi:10.1029/2010GL042652, 2010.

Haas, C., and Howell, S. E. L.: Ice thickness in the Northwest Passage, Geophys. Res. Lett., 42, 7673–7680, doi:10.1002/2015GL065704, 2015.

520 Hernández-Henríquez, M., Déry, S., and Derksen, C.: Polar amplification and elevation-dependence in trends of Northern Hemisphere snow cover extent, 1971-2014, Env. Res. Lett., 10, doi:10.1088/1748-9326/10/4/044010, 2015.

Hochheim, K. P., and Barber, D. G.: An update on the ice climatology of the Hudson Bay system, Arct Antarct Alp Res., 46, 66–83,doi:10.1657/1938-4246-46.1.66, 2014.

Hodson, D., Keeley, S., West, A., Ridley, J., Hawkins, E., and Hewitt, H.: Identifying uncertainties in Arctic climate change
525 projections. Clim. Dyn., DOI: 10.1007/s00382-012-1512-z, 2012.

Hori, M., Sugiura, K., Kobayashi, K., Aoki, T., Tanikawa, T., Kuchiki, K., Niwano, M., and Enomoto, H.: A 38-year (1978–2015) Northern Hemisphere daily snow cover extent product derived using consistent objective criteria from satellite-borne optical sensors. Remote Sens. Environ., 191, 402–418, Doi:10.1016/j.rse.2017.01.023, 2017.

Howell, S. E. L., Duguay, C. R., and Markus, T.: Sea ice conditions and melt season duration variability within the Canadian
530 Arctic Archipelago: 1979–2008, Geophys. Res. Lett., 36, L10502, doi:10.1029/2009GL037681, 2009.

Howell, S. E. L., Wohlleben, T., Dabboor, M., Derksen, C., Komarov, A., and Pizzolato, L.: Recent changes in the exchange of sea ice between the Arctic Ocean and the Canadian Arctic Archipelago, J. Geophys. Res. Oceans, 118, 3595–3607, doi:10.1002/jgrc.20265, 2013a.

Howell, S. E. L., Wohlleben, T., Komarov A., Pizzolato L., and Derksen, C.: Recent extreme light sea ice years in the
535 Canadian Arctic Archipelago: 2011 and 2012 eclipse 1998 and 2007, Cryosphere, 7(6), 1753–1768, doi:10.5194/tc-7-1753-2013, 2013b.Howell, S. E. L., Derksen, C.,Pizzolato, L., and Brady, M.: Multiyear ice replenishment in the Canadian Arctic Archipelago: 1997–2013, J. Geophys. Res. Oceans, 120, 1623–1637, doi:10.1002/2015JC010696, 2015.

Howell, S. E. L., Brady, M., Derksen, C., and Kelly, R. E. J.: Recent changes in sea ice area flux through the Beaufort Sea during the summer, J. Geophys. Res. Oceans, 121, 2659–2672, doi:10.1002/2015JC011464, 2016.

540   Howell, S.E.L., Laliberté, F., Kwok, R., Derksen, C., and King, J.: Landfast ice thickness in the Canadian Arctic Archipelago from Observations and Models, The Cryosphere, 10, doi:10.5194/tc-10-1463-2016, 2016.

Kobayashi, S., Y. Ota, Y. Harada, A. Ebita, M. Moriya, H. Onoda, K. Onogi, H. Kamahori, C. Kobayashi, H. Endo, K. Miyaoka, and K. Takahashi: The JRA-55 Reanalysis: General specifications and basic characteristics. J. Meteor. Soc. Japan, 93, 5-48, doi:10.2151/jmsj.2015-001, 2015.

545   Krishfield, R. A., Proshutinsky, A., Tateyama, K., Williams, W. J., Carmack, E. C., McLaughlin, F. A. and Timmermans, M.-L.: Deterioration of perennial sea ice in the Beaufort Gyre from 2003 to 2012 and its impact on the oceanic freshwater cycle, J. Geophys. Res. Oceans, 119, 1271–1305, doi:10.1002/2013JC008999, 2014.

Kunkel, K., Robinson, D., Champion, S., Yin, X., Estilow, T., and Frankson, R.: Trends and Extremes in Northern Hemisphere Snow Characteristics, Curr Clim Change Rep., 2, 65–73, DOI 10.1007/s40641-016-0036-8, 2017.

550   Kushner, P. J., Mudryk, L. R., Merryfield, W., Ambadan, J. T., Berg, A., Bichet, A., Brown, R., Derksen, C. P., Déry, S. J., Dirkson, A., Flato, G., Fletcher, C. G., Fyfe, J. C., Gillett, N., Haas, C., Howell, S., Laliberté, F., McCusker, K., Sigmond, M., Sospreda-Alfonso, R., Tandon, N. F., Thackeray, C., Tremblay, B., and Zwiers, F. W.: Assessment of snow, sea ice, and related climate processes in Canada's Earth-System Model and Climate Prediction System, The Cryosphere Discuss., https://doi.org/10.5194/tc-2017-157, in review, 2017.

555   Kwok, R., and Rothrock, D. A.: Decline in Arctic sea ice thickness from submarine and ICESat records: 1958 – 2008, Geophys. Res. Lett., 36, L15501, doi:10.1029/2009GL039035, 2009.

Kwok, R., and Cunningham, G. F.: Contribution of melt in the Beaufort Sea to the decline in Arctic multiyear sea ice coverage: 1993–2009, Geophys. Res. Lett., 37, L20501, doi:10.1029/2010GL044678, 2010.

Kwok, R., and Cunningham, G. F.: Variability of Arctic sea ice thickness and volume from CryoSat-2, Philos. Trans. R.
560   Soc., A, 373,20140157, doi:10.1098/rsta.2014.0157, 2015.

Laliberté, F., Howell, S. E. L., and Kushner, P.J.: Regional variability of a projected sea ice-free Arctic during the summer months, Geophys. Res. Lett., 43, doi:10.1002/2015GL066855, 2016.

Laxon S. W., Giles, K. A., Ridout, A. L., Wingham, D. J., Willatt, R., Cullen, R., Kwok, R., Schweiger, A., Zhang, J., Haas, C., Hendricks, S. Krishfield, R., Kurtz, N., Farrell, S., and Davidson, M.: CryoSat-2 estimates of Arctic sea ice thickness and
565   volume, Geophys. Res. Lett., 40, 732–737, doi:10.1002/grl.50193, 2013.

Maslanik, J., Stroeve, J., Fowler, C., and Emery, W.: Distribution and trends in Arctic sea ice age through spring 2011, Geophys. Res. Lett., 38, L13502, doi:10.1029/2011GL047735, 2011.

Mudryk, L., Kushner, P., and Derksen, C.: Interpreting observed Northern Hemisphere snow trends with large ensembles of climate simulations, Clim. Dyn., 43, 345–359, DOI 10.1007/s00382-013-1954-y, 2014.

570   Mudryk, L., Derksen, C., Kushner, P., and Brown, R.: Characterization of Northern Hemisphere snow water equivalent datasets, 1981–2010, J. Clim., 28, 8037-8051, 2015.

Mudryk, L. R., Kushner, P. J., Derksen, C., and Thackeray, C.: Snow cover response to temperature in observational and climate model ensembles, Geophys. Res. Lett., 44, doi:10.1002/2016GL071789, 2017.

Notz, D., and Stroeve, J.:Observed Arctic sea-ice loss directly follows anthropogenic CO2 emission, Science,
575   10.1126/science.aag2345, 2016.

Onogi, K., J. Tsutsui, H. Koide, M. Sakamoto, S. Kobayashi, H. Hatsushika, T. Matsumoto, N. Yamazaki, H. Kamahori, K. Takahashi, S. Kadokura, K. Wada, K. Kato, R. Oyama, T. Ose, N. Mannoji and R. Taira: The JRA-25 Reanalysis. J. Meteor. Soc. Japan, 85, 369-432, 2007.

Parkinson, C. L.: Spatially mapped reductions in the length of the Arctic sea ice season, Geophys. Res. Lett., 41, 4316–4322,
580   doi:10.1002/2014GL060434, 2014.

Peters, G. P., et al. : The challenge to keep global warming below 2 °C. Nat. Clim. Chang., 3, 4–6, doi:10.1038/nclimate1783.

Pithan, F., and Mauritsen, T.: Arctic amplification dominated by temperature feedbacks in contemporary climate models. Nature Geoscience, 7, 181-184, doi:10.1038/ngeo2071, 2014.

585   Pizzolato, L., Howell, S. E. L., Dawson, J., Laliberté, F., and Copland, L.: The influence of declining sea ice on shipping activity in the Canadian Arctic, Geophys. Res. Lett., 43, doi:10.1002/2016GL071489, 2016.

Quadrelli, R., and Wallace, J.: Dependence of the structure of the Northern Hemisphere annular mode on the polarity of ENSO, Geophys. Res. Lett., 29, 2132-2135, doi:10.1029/2002GL015807, 2002.

Raisanen, J.: Warmer climate: less or more snow? Clim. Dyn., 30, 307-319, 2008.

590   Rapaic, M., Brown, R., Markovic M., and Chaumont, D.: An evaluation of temperature and precipitation surface-based and reanalysis datasets for the Canadian Arctic, 1950-2010. Atmosphere-Ocean, 53, 283-303, doi:10.1080/07055900.2015.1045825, 2015.

Reichle, R., Draper, C., Liu, Q., Girotto, M., Mahanama, S., Koster, R., and De Lannoy, G.: Assessment of MERRA-2 land surface hydrology estimates, J. Clim., 30, DOI: 10.1175/JCLI-D-16-0720.1, 2017.

595   Richter-Menge, J. A., and Farrell S. L.: Arctic sea ice conditions in spring 2009-2013 prior to melt, Geophys. Res. Lett., 40, 5888–5893, doi:10.1002/2013GL058011, 2013.

Rienecker, M. M., et al.: MERRA: NASA's Modern-Era Retrospective Analysis for Research and Applications. J. Clim., 24, 3624–3648, doi:10.1175/JCLI-D-11-00015.1, 2011.

Rigor, I. G., Wallace, J. M., and Colony, R. L.: Response of sea ice to the Arctic oscillation, J. Clim., 15(18), 2648–2663,
600   doi:10.1175/1520-0442(2002)015<2648:ROSITT>2.0.CO;2, 2002.

Saha, S., S. Moorthi, H. Pan, X. Wu, J. Wang, S. Nadiga, P. Tripp, R. Kistler, J. Woollen, D. Behringer, H. Liu, D. Stokes, R. Grumbine, G. Gayno, J. Wang, Y. Hou, H. Chuang, H.H. Juang, J. Sela, M. Iredell, R. Treadon, D. Kleist, P. Van Delst, D. Keyser, J. Derber, M. Ek, J. Meng, H. Wei, R. Yang, S. Lord, H. Van Den Dool, A. Kumar, W. Wang, C. Long, M. Chelliah, Y. Xue, B. Huang, J. Schemm, W. Ebisuzaki, R. Lin, P. Xie, M. Chen, S. Zhou, W. Higgins, C. Zou, Q. Liu, Y.
605   Chen, Y. Han, L. Cucurull, R.W. Reynolds, G. Rutledge, and M. Goldberg: The NCEP Climate Forecast System Reanalysis. Bull. Amer. Meteor. Soc., 91, 1015–1057, doi: 10.1175/2010BAMS3001.1, 2010.Scalzitti, J., Strong, C., and Kochanski, A.: Climate change impact on the roles of temperature and precipiation in western U.S. snowpack variability, Geophys. Res. Lett., 43, 5361—5369, 2016.

Scaife, A. A., and Coauthors,: Improved Atlantic winter blocking in a climate model. *Geophys. Res. Lett.*, **38**, L23703,
610   doi:10.1029/2011GL049573, 2011.

Screen, J., Deser, C., and Sun, L.: Reduced risk of North American cold extremes due to continued Arctic sea ice loss, Bull. Am. Met. Soc., DOI:10.1175/BAMS-D-14-00185.1, 2015.

Serreze, M., Barrett, A., Stroeve, J., Kindig, D., and Holland, M.: The emergence of surface-based Arctic amplification, Cryos., 3, 11–19, 2009.

615   Serreze, M., Barrett, A., Slater, A., Steele, M., Zhang, J., and Trenberth, K. The large-scale energy budget of the Arctic. J. Geophys. Res., 112: D11122, doi:10.1029/2006JD008230, 2007.

Smith, K.L., C.G. Fletcher, and P.J. Kushner: The Role of Linear Interference in the Annular Mode Response to Extratropical Surface Forcing. *J. Climate,* **23**, 6036–6050, doi:10.1175/2010JCLI3606.1,2010.

Sospedra-Alfonso R., Melton J., and Merryfield, W.: Effects of temperature and precipitation on snowpack variability in the
620   central Rocky Mountains as a function of elevation. Geophys. Res. Lett., 42, 4429–4438, 2015.

Sospedra-Alfonso, R. and Merryfield, W. J.: Influences of temperature and precipitation on historical and future snowpack variability over the Northern Hemisphere in the Second-Generation Canadian Earth System Model, J.Clim., in press, 2017.

Stroeve, J. C., Markus, T., Boisvert, L., Miller, J., and Barrett, A.: Changes in Arctic melt season and implications for sea ice loss, Geophys. Res. Lett., 41(4), 1216–1225, doi:10.1002/2013GL058951, 2014.

625   Sturm, M., Goldstein, M., Huntington, H., and Douglas, T.: Using an option pricing approach to evaluate strategic decisions in a rapidly changing climate: Black–Scholes and climate change. Clim. Change, DOI 10.1007/s10584-016-1860-5, 2016.

Sturm, M., Goldstein, M. A., and Parr, C.: Water and life from snow: A trillion dollar science question, Water Resour. Res., 53, doi:10.1002/ 2017WR020840, 2017.

Takala, M., Luojus, K., Pulliainen, J., Derksen, C., Lemmetyinen, J., Kärnä, J-P, and Koskinen, J.: Estimating northern

630   hemisphere snow water equivalent for climate research through assimilation of space-borne radiometer data and ground-based measurements, Remote Sens. Environ., 115, 3517–3529, doi:10.1016/j.rse.2011.08.014, 2011.

Thackeray, C. W., Fletcher, C. G,. Mudryk, L. R., and Derksen, C.: Quantifying the uncertainty in historical and future simulations of Northern Hemisphere spring snow cover, J. Clim., 29(23), 8647–8663, doi:10.1175/JCLI-D-16-0341.1, 2016.

Tucker, W. B., III, Weatherly, J. W., Eppler, D. T., Farmer, L. D., and Bentley, D. L., Evidence for rapid thinning of sea ice

635   in the western Arctic Ocean at the end of the 1980s, Geophys. Res. Lett., 28(14), 2851–2854, doi:10.1029/2001GL012967, 2001.

Tilling, R. L., Ridout, A., Shepherd, A., and Wingham, D. J.: Increased Arctic sea ice volume after anomalously low melting in 2013, Nat. Geosci., 8(8), 643–646, doi:10.1038/ngeo2489, 2015.

Tivy, A., Howell, S. E. L., Alt, B., McCourt, S., Chagnon, R., Crocker, G., Carrieres, T., and Yackel, J.: Trends and

640   variability in summer sea ice cover in the Canadian Arctic based on the Canadian Ice Service Digital Archive, 1960–2008 and 1968–2008, J. Geophys. Res., 116, C03007, doi:10.1029/2009JC005855, 2011a.

Tivy A, Howell, S.E.L., Alt, B, Yackel J.J., and Carrieres, T.: Origins and levels of seasonal forecast skill for sea ice

in Hudson Bay using Canonical Correlation Analysis. J Clim 24. doi:10.1175/2010JCLI3527.1, 2011b.

van den Hurk, B., Kim, H., Krinner, G., Seneviratne, S., Derksen, C., Oki, T., Douville, H., Colin, J., Ducharne, A., Cheruy

645   F., Viovy, N., Puma, M., Wada, Y., Li, W., Jia , B., Alessandri, A., Lawrence, D., Weedon, G., Ellis, R., Hagemann, S., Mao, J., Flanner, M., Zampieri, M., Law, R., and Sheffield, J. :. LS3MIP (v1.0) contribution to CMIP6: The Land Surface, Snow and Soil moisture Model Intercomparison Program – aims, set-up and expected outcome. Geophys. Mod. Dev., 9, 2809–2832, 2016.

Vincent, L. Zhang, X., Brown, R., Feng, Y., Mekis, E. Milewska, E., Wan, H., and Wang, X.: Observed trends in Canada's

650   climate and influence of low-frequency variability modes, J. Clim., 28, 4545-4560, 2015.

Table 1: List of CMIP5 models (with number of realizations) used for terrestrial snow analysis of both historical and future periods.

Model	No.
BCC-CSM1.1	1
BNU-ESM	1
CanESM2	5
CCSM4	6
CNRM-CM5	5
CSIRO-Mk3.6.0	10
FGOALS-g2	1
GISS-E2-R	1
INM-CM4	1
MIROC5	3
MIROC-ESM	1
MPI-ESM-LR	3
MRI-CGCM3	1
NorESM1-ME	1
NorESM1-M	1

655

Table 2: List of CMIP5 models (with number of realizations) used for sea ice analysis of both historical and future periods.

Model	No.	Model	No.
BCC-CSM1-1	1	MIROC5	3
BCC-CSM-1-m	1	HadGEM2-CC	1
BNU-ESM	1	HadGEM2-ES	4
CanESM2	5	MPI-ESM-LR	3
CMCC-CESM	1	MPI-ESM-MR	1
CMCC-CM	1	MRI-CGCM3	1
CMCC-CMS	1	MRI-ESM1	1
CNRM-CM5	5	GISS-E2-H	1
ACCESS1.0	1	GISS-E2-H-CC	1
ACCESS1.3	1	GISS-E2-R	5
CSIRO-Mk3.6.0	10	GISS-E2-R-CC	1
FIO-ESM	1	CCSM4	6
EC-EARTH	11	NorESM1-M	1
inmcm4	1	NorESM1-ME	1
IPSL-CM5A-LR	4	HadGEM2-AO	1
IPSL-CM5A-MR	1	GFDL-CM3	1
IPSL-CM5B-LR	1	GFDL-ESM2G	1
FGOALS-g2	1	GFDL-ESM2M	1
FGOALS-s2	1	CESM1(BGC)	1
MIROC-ESM	1	CESM1(CAM5)	3
MIROC-ESM-CHEM	1	CESM1-CAM5-1-FV2	1

660
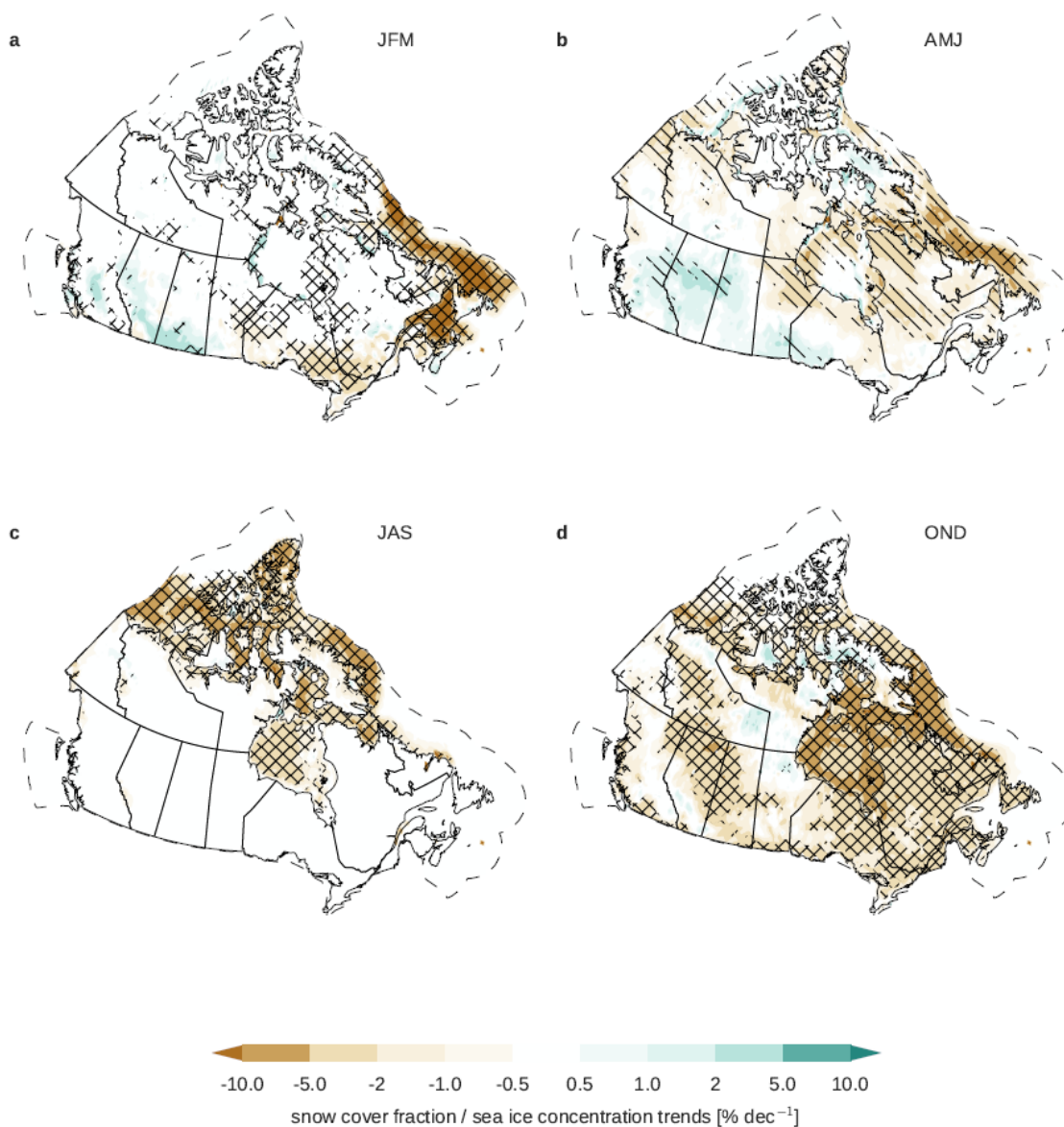
Figure 1: Terrestrial snow cover fraction and sea ice concentration trends for 1981-2015. Datasets are described in Section 2.1. Single hatching (\) indicates pointwise significance at the 90th percentile. Crossed hatching (X) means False Discovery Rate (FDR) significance at the 90th percentile (Wilks 2006, after excluding regions with non-varying cover). A pointwise significant location is always FDR significant. Dashed line denotes limit of Canadian marine territory.
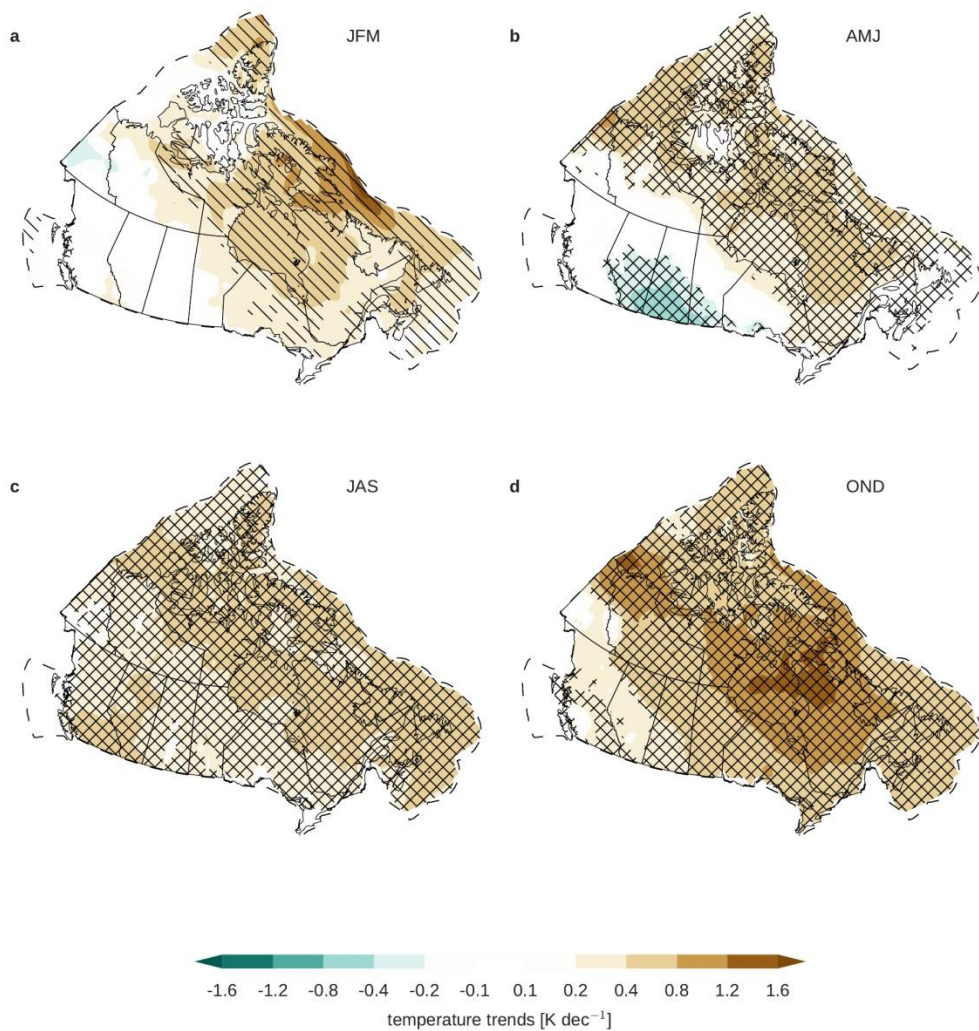
670   **Figure 2: Trends in surface temperature, 1981-2015, from a blend of ERA-Interim, JRA-55, JRA-25, MERRA1, MERRA2, and CFSR reanalysis products. See Figure 1 for explanation of hatching.**
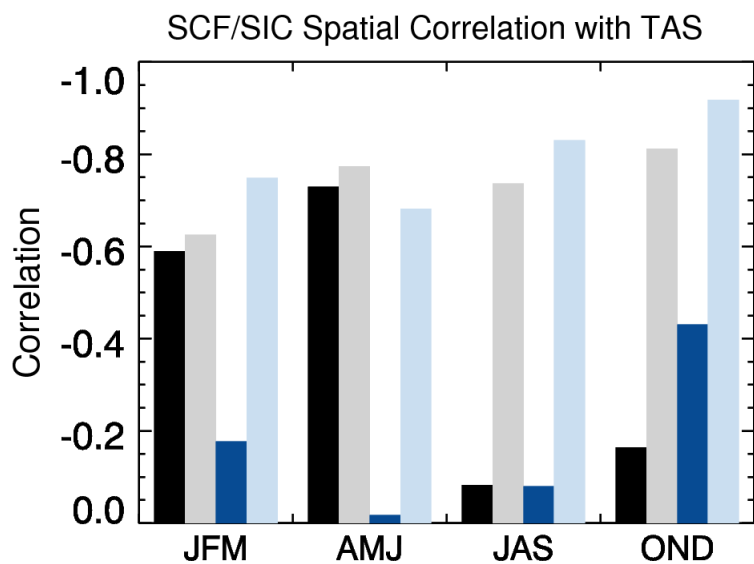
Figure 3: Centered (dark) or uncentered (light) pattern correlation between seasonal TAS trends and seasonal SCF (black) or SIC (blue) trends.
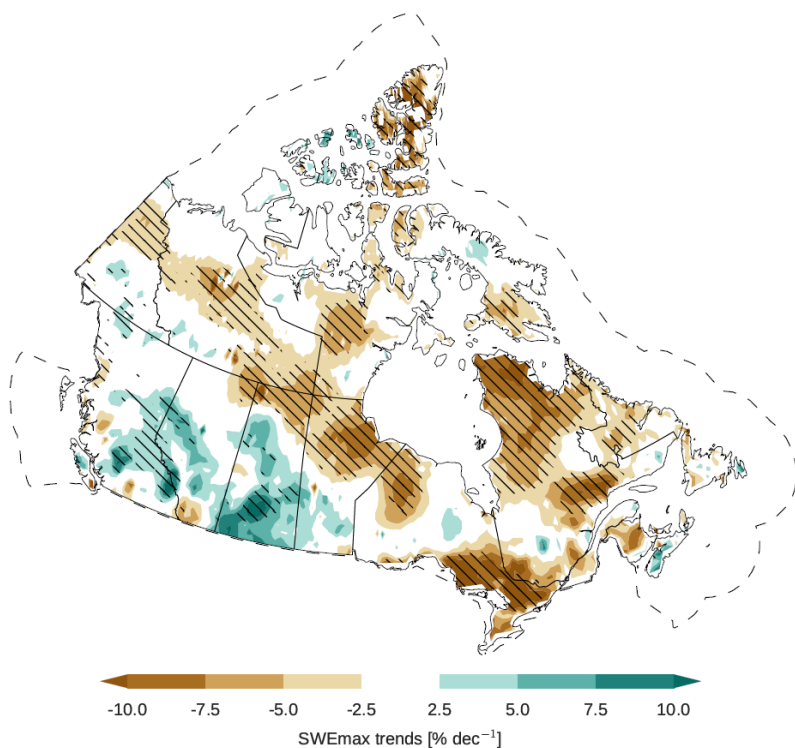
Figure 4: SWEmax trends for 1981-2015 (see Figure 1 for explanation of hatching)

680
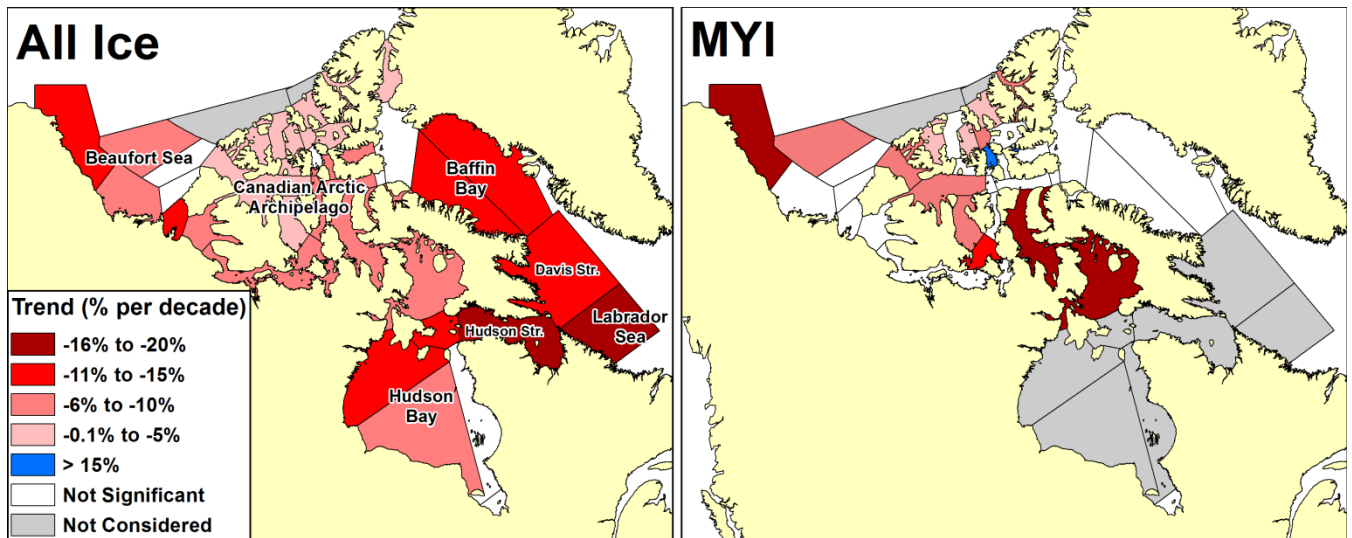
Figure 5: Trends in summer all ice (left) and multi-year ice (right) area from 1968 to 2016 from the CISDA. Only trends significant to the 95% confidence level are shown.
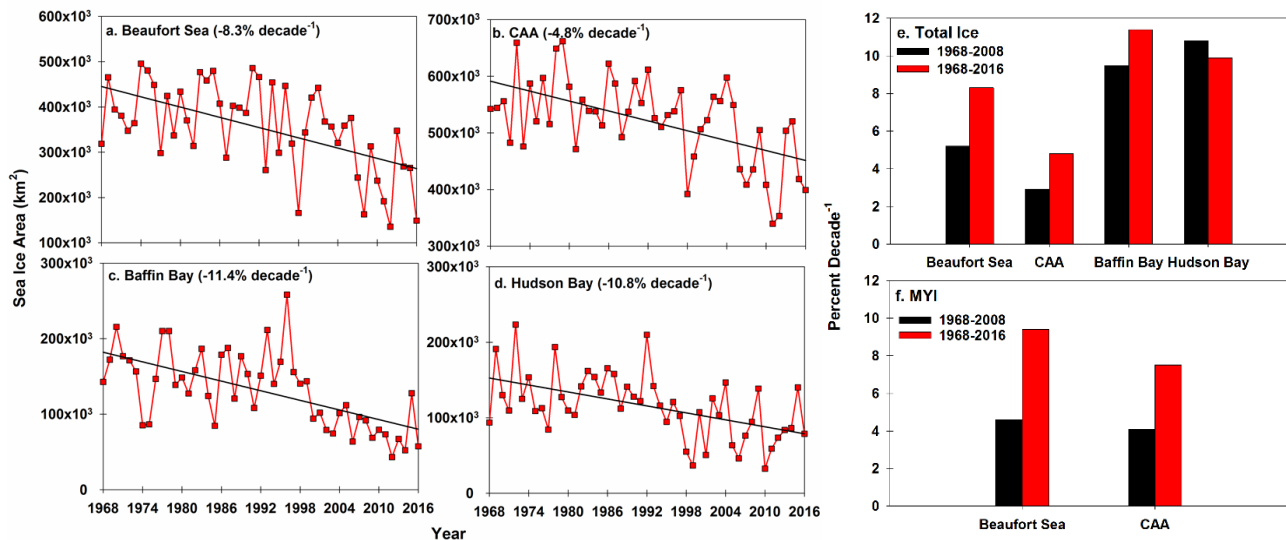
685 **Figure 6: Time series of summer total sea ice area for the (a) Beaufort Sea, (b) Canadian Arctic Archipelago (CAA), (c) Baffin Bay and (d) Hudson Bay regions from 1968 to 2016. Comparison of trends between 1968-2008 and 1968-2016 for all ice (e) and multi-year ice (MYI) (f) for selected regions in the Canadian Arctic.**
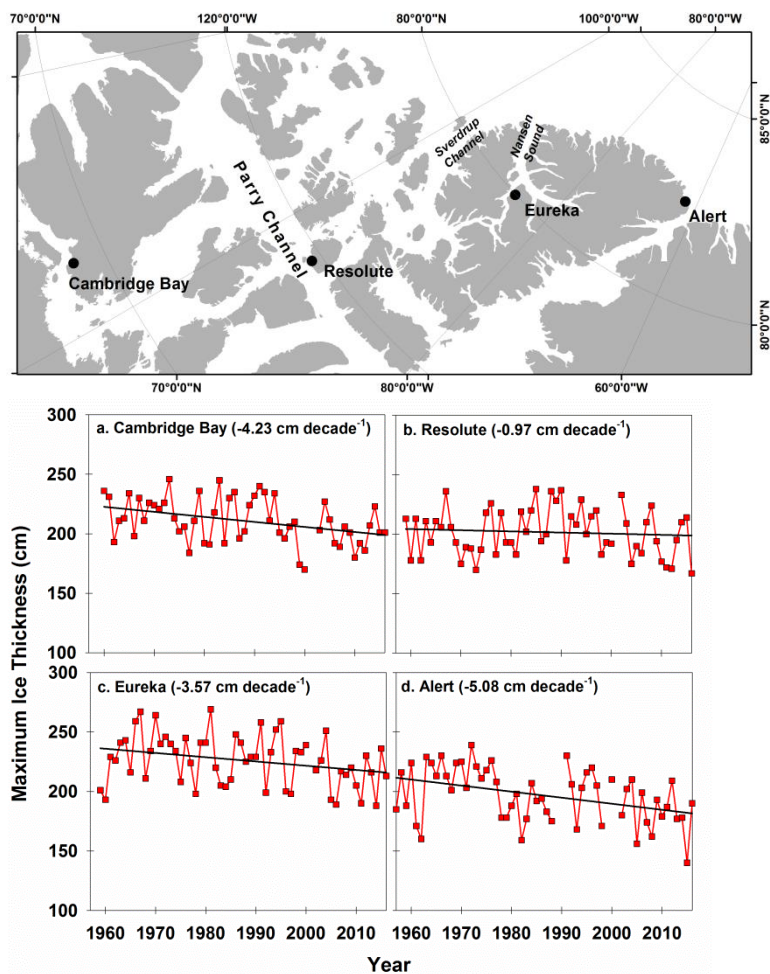
690

Figure 7: Time series and trend of observed maximum ice thickness at (a) Cambridge Bay, (b) Resolute, (c) Eureka and (d) Alert locations in the Canadian Arctic.
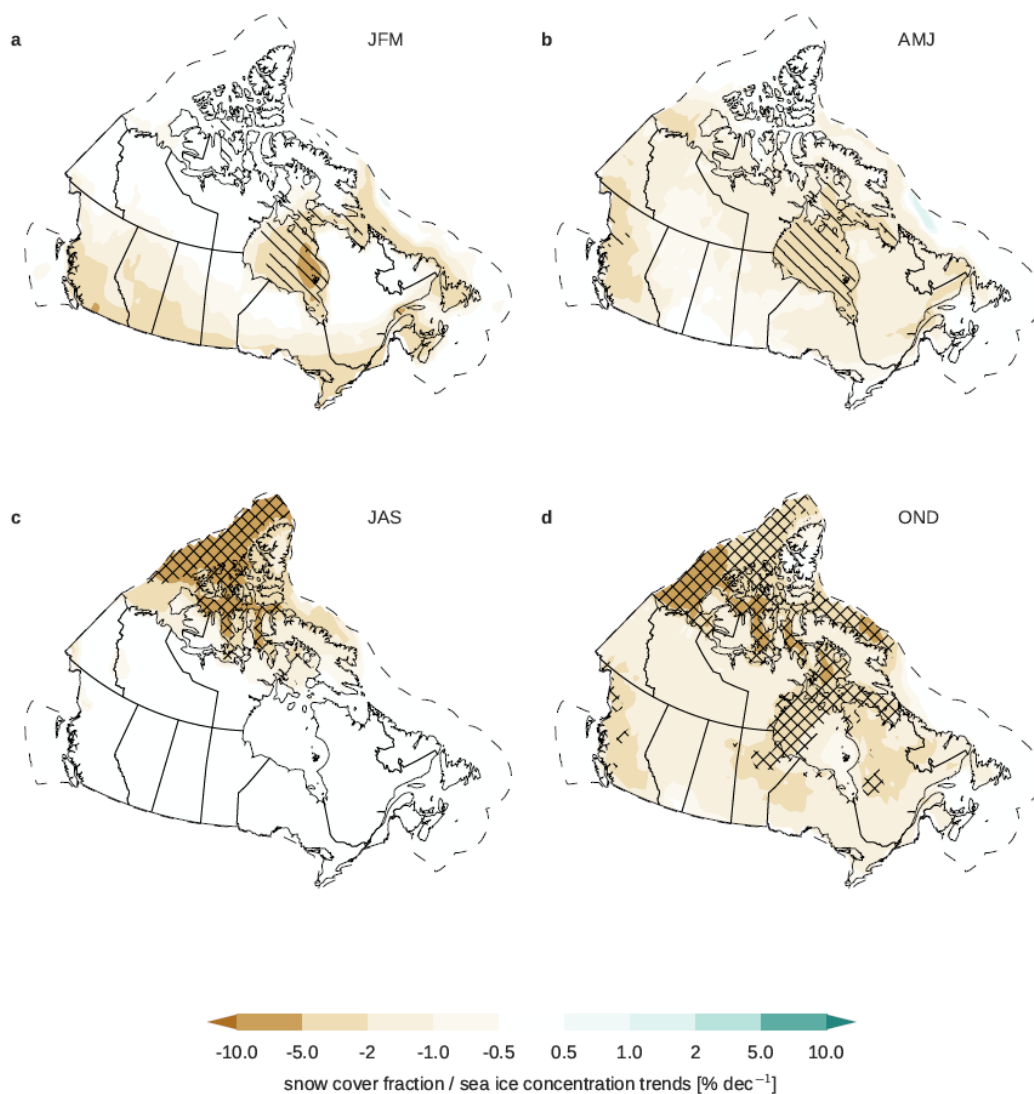
695

Figure 8: Projected terrestrial snow cover fraction and sea ice concentration trends for 2020-2050. Model simulations are described in Section 2.2. See Figure 1 for explanation of hatching.
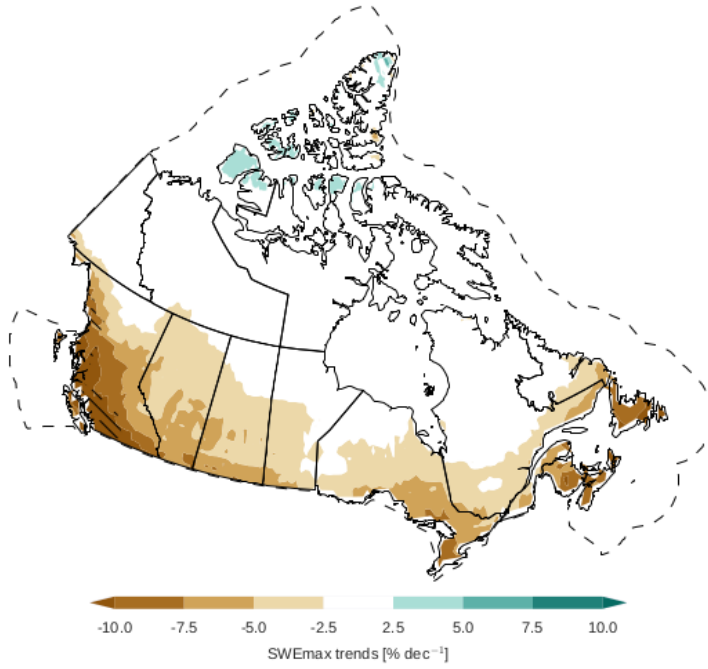
Figure 9: 2020-2050 trends in SWEmax from the CMIP5 ensemble. See Figure 1 for explanation of hatching. We show percent change relative to the climatological (1981-2015) mean because there is large variability in SWEmax across the country (high SWE in western cordillera; low SWE in the Prairies).
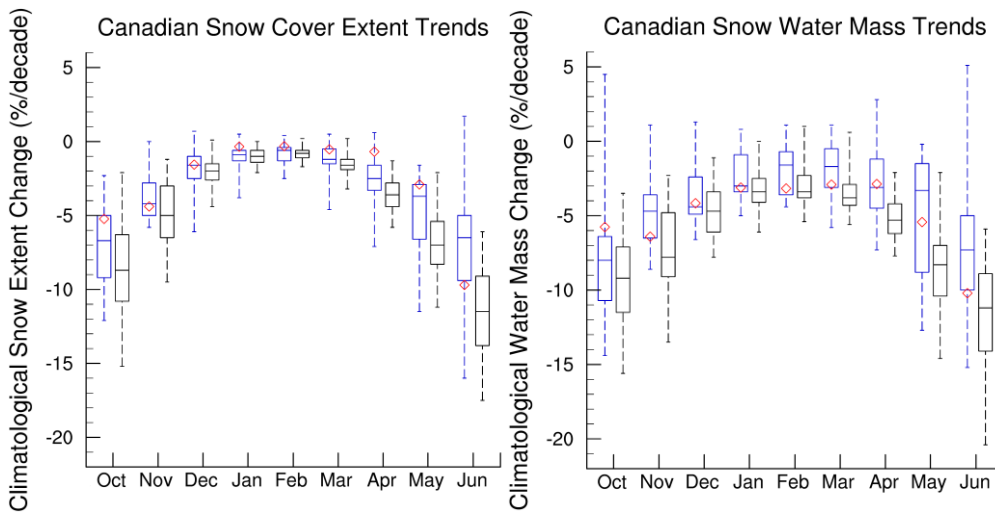
Figure 10: 2020-2050 monthly trends in Canadian snow cover extent (left) and snow water mass (right) from the CMIP5 multimodel ensemble (blue) and CanESM large initial condition ensemble (black). Monthly mean observational trends (1981-2015) from the snow dataset used in Section 2 are shown in red. For each box the enclosed region shows the 25th-75th percentile range, the horizontal line shows the median, and the dashed whiskers illustrate the minimum and maximum.
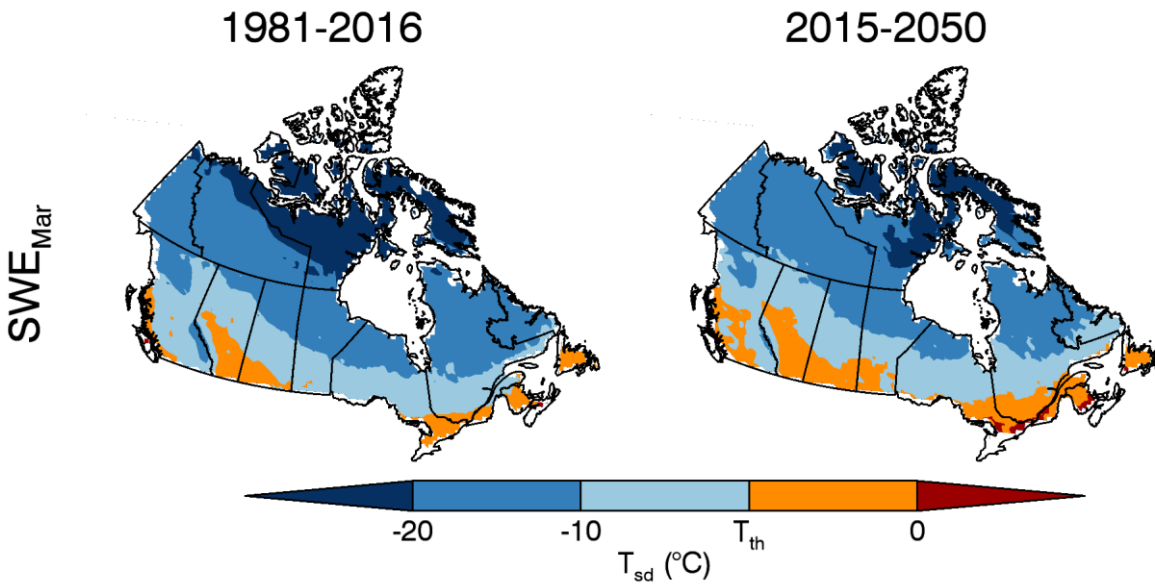
710

Figure 11: Projected temperature and precipitation controls on changes in March snow water equivalent, 1981-2016 (left); projection to 2050 (right).
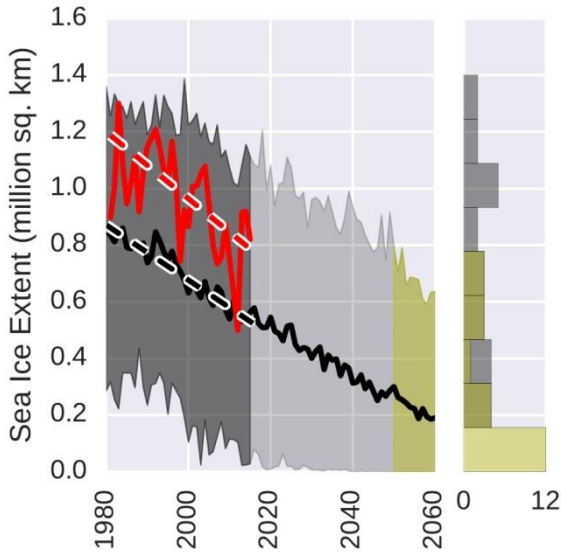
715 **Figure 12: Observed (red line) sea ice extent over Canadian marine regions (SIC > 0.15); CMIP-5 multi-model mean (black line) and spread (shading). Histogram on the right shows the model distribution for 1980-2015 in black and for 2050-2060 in yellow.**
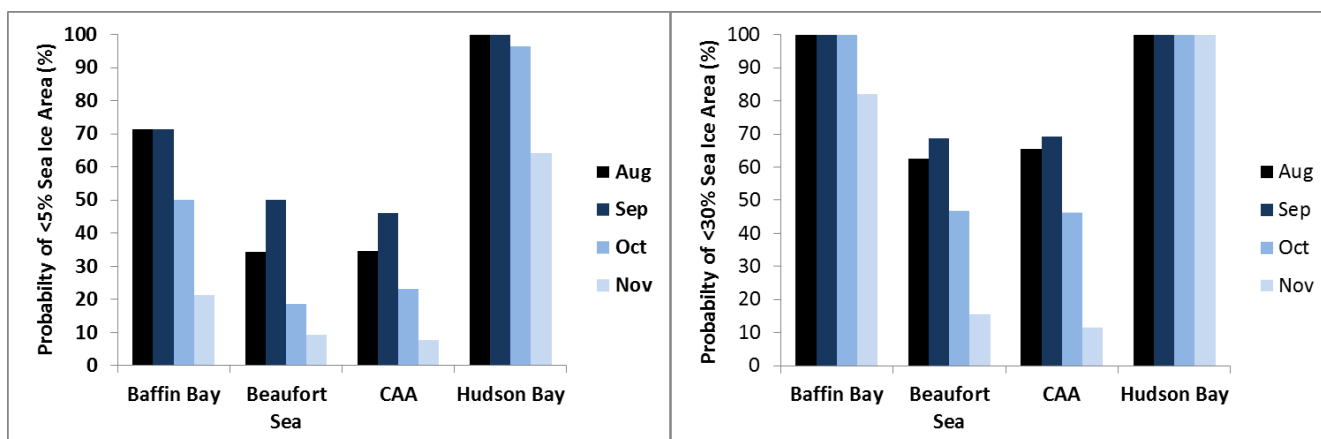
720   **Figure 13: Probability of sea ice free conditions by 2050 from the CMIP5 multi-model mean using a 5% (left) and 30% (right) sea ice area threshold.**